

Sensitized Emission of Luminescent Lanthanide Complexes Based on a Phosphane Oxide Derivative[†]

Minh-Huong Ha-Thi,^{*,‡} Jacques Alexis Delaire,[‡] Véronique Michelet,[§] and Isabelle Leray^{*,‡}

PPSM, ENS Cachan, CNRS, UniverSUD Paris, 61 Av Président Wilson, F-94230 Cachan, and Laboratoire Charles Friedel, E.N.S.C.P., UMR7223, 11 rue P. et M. Curie, 75231 Paris, Cedex 05, France

Received: September 30, 2009; Revised Manuscript Received: November 27, 2009

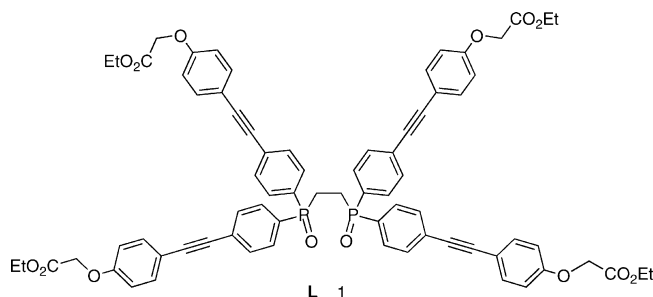
The photophysical properties of a complex based on diphenylphosphanoethane (DPPE) fluorescent ligands linked to a europium ion have been investigated by different spectroscopic methods. Upon complexation with europium, the interaction of the phosphane oxide group with europium leads to a red shift of the absorption spectrum and a strong quenching of the ligand emission. The typical sensitized emission of Eu^{3+} is observed upon excitation of the ligand with a fluorescence quantum yield of 1%. Time-resolved absorption and emission experiments have been performed in order to investigate the photophysical mechanism involved in this complex. Photophysical studies show that an energy-transfer mechanism occurs from both the first excited singlet and triplet states of the ligand, and the population of the europium ion to the $^5\text{D}_1$ state takes place, from which the $^5\text{D}_0$ state is populated. Additionally, electron transfer from the excited singlet state of the ligand to the europium ion appears as a very efficient process.

1. Introduction

Over the past few decades, considerable attention has been devoted to the design of lanthanide complexes due to their very attractive properties and their potential applications as emitters in organic-light-emitting diodes (OLED) as well as molecular probes for biological imaging and sensing.^{1,2} Due to the forbidden character of the intra-4f transitions, the lanthanides exhibit very low absorption coefficients, and considerable efforts have been directed to the design of new chromophores able to sensitize the lanthanides efficiently.^{3,4} Among the complexing units, it has been demonstrated that the skeleton based on a phosphane oxide group can strongly coordinate europium ions,⁵ and several europium complexes containing these key functional groups as ligands have been synthesized.^{6–9} Moreover phosphane oxide based derivatives offer several advantages in terms of high fluorescence quantum yields.¹⁰

We have recently been involved in the design of new fluorescent probes and have described the synthesis and the photophysical properties of new fluorophores and fluorescent molecular sensors bearing phosphane oxide^{11–13} and phosphane sulfide groups.^{14–16} These fluorophores show very high absorption coefficients and efficiently complex cations such as heavy metal ions. Taking advantages of the complexing abilities of the P=O group with europium, we decided to synthesize the ligand **L1** consisting of diphenylphosphanoethane derivative (Scheme 1) and to evaluate the photophysical properties of the complex of **L1** with Eu^{3+} .^{17,18} Especially, we have been interested in investigating by different photophysical methods (absorption, time-resolved fluorescence, and transient absorption measurements) the involved mechanism in the energy-transfer process from the ligand to the europium ion.

SCHEME 1: Structure of the Ligand L1



2. Experimental Section

Synthesis. The phosphane oxide **3** was prepared according to previously described procedures.¹³ To a solution of **3** (100 mg, 0.19 mmol) in toluene (30 mL) and triethylamine (8 mL), 377 mg of **4** (1.23 mmol) was added. The mixture was degassed under argon, and CuI (8.7 mg, 0.04 mmol) and $\text{Pd}(\text{PPh}_3)_4$ (26 mg, 0.02 mmol) were added. The reaction mixture was then stirred for 20 h at 50 °C under argon. The volatiles were evaporated under vacuum, and the residue was dissolved in dichloromethane (10 mL). The organic layer was washed with aqueous HCl (10%), dried (Na_2SO_4), and filtered, and the solvents were evaporated under reduced pressure. The crude product was then purified by flash chromatography (Silica gel: CH_2Cl_2 100% to CH_2Cl_2 -acetone: 1/1) to afford the desired ligand **L1** (130 mg, 56% yield) as a white solid. ^1H NMR (CDCl_3 , 300 MHz): δ (ppm) = 1.30 (t, J = 7.35 Hz, 12H), 2.51 (m, 4H), 4.27 (q, J = 7 Hz, 8H), 4.64 (s, 8H), 6.88 (d, J = 8.8 Hz, 8H), 7.47 (d, J = 8.8 Hz, 8H), 7.5–7.7 (m, 16H). ^{13}C NMR (CDCl_3 , 75 MHz): δ (ppm) = 14.3 (CH_3), 61.6 (CH_2), 65.5 (CH_2), 87.5, 92.4 ($\text{C}'\text{C}$), 114.9 (CH_{ar}), 116.0 (C_{ar}), 127.9 (C_{ar}), 130.8 (CH_{ar}), 131.9 (CH_{ar}), 133.5 (CH_{ar}), 158.4 (C_{ar} -O), 168.6 ($\text{C}=\text{O}$). ^{31}P NMR (CDCl_3 , 121 MHz): δ (ppm) = 32.3. HRMS (MALDI): m/z : calcd for $\text{C}_{74}\text{H}_{65}\text{O}_{14}\text{P}_2$: 1239.3844; found: 1239.3800 [$\text{M}+\text{H}$]⁺. The complex ML_3 was formed in situ by

[†] Part of the “Benoît Soep Festschrift”.

^{*} To whom correspondence should be addressed. E-mail: minh-huong.ha-thi@u-psud.fr (M.-H.H.-T.); Isabelle.Leray@ppsm.ens-cachan.fr (I.L.).

[‡] UniverSUD Paris.

[§] E.N.S.C.P.

mixing typically $4 \times 10^{-6} \text{ mol} \cdot \text{L}^{-1}$ of Eu^{3+} with $1.2 \times 10^{-5} \text{ mol} \cdot \text{L}^{-1}$ of ligand.

Solvents and Salts. Acetonitrile and chloroform from Aldrich (spectrometric grade) were used as solvents for the absorption and fluorescence measurements. Europium nitrate or terbium nitrate from Aldrich or Alfa Aesar was of the highest quality available and vacuum-dried over P_2O_5 prior to use.

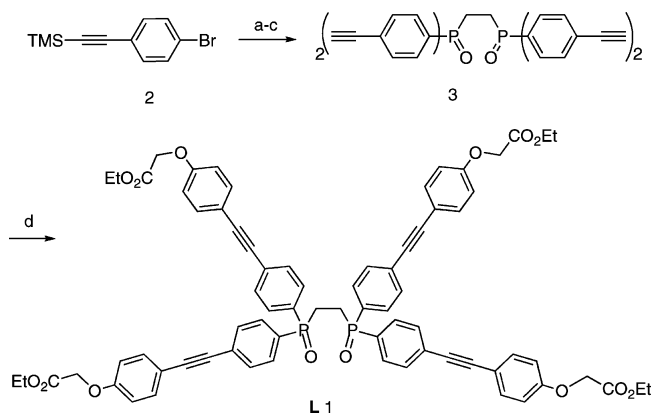
Spectroscopic Measurements. UV/vis absorption spectra were recorded on a Varian Cary5E spectrophotometer, and corrected emission spectra were obtained on a Jobin-Yvon Spex Fluorolog 1681 spectrofluorimeter. The fluorescence quantum yields were determined by using either quinine sulfate dihydrate in sulfuric acid, 0.5 N ($\Phi_{\text{F}} = 0.546^{19}$), or $[\text{Ru}(\text{bipy})_3]\text{Cl}_2$ in water ($\Phi_{\text{F}} = 0.028^{20}$) as standards. The complexation equilibrium constants were determined by global analysis of the evolution of all absorption and/or emission spectra by using the Specfit Global Analysis System V3.0 for a 32 bit Windows system. This software uses singular value decomposition and nonlinear regression modeling by the Levenberg–Marquardt method.²¹ Fluorescence intensity decays were obtained by the single-photon timing method with picosecond laser excitation with a Spectra–Physics setup composed of a titanium sapphire Tsunami laser pumped by an argon ion laser, a pulse detector, and doubling (LBO) and tripling (BBO) crystals. Light pulses were selected by an optoacoustic crystal at a repetition rate of 4 MHz. Fluorescence photons were detected through a long-pass filter (375 nm) by means of a Hamamatsu MCP R3809U photomultiplier, connected to a constant-fraction discriminator. The time-to-amplitude converter was purchased from Tennelec. Data were analyzed by a nonlinear least-squares method with the aid of Globals software (Globals Unlimited, University of Illinois at Urbana–Champaign, Laboratory of Fluorescence Dynamics).

Transient absorption measurements were carried out by nanosecond laser flash photolysis. The setup used the third harmonics of a Q-switched Nd:YAG laser by BM Industries (model BMI 5011 DNS 10), delivering 7–8 ns pulses at 1064 nm. Q-switching was achieved with a Pockels cell inside of the cavity. The giant pulse was frequency-doubled and -tripled in KDP crystals. The output energy was 50 mJ at 355 nm. The energy deposited in the sample was lowered to 3 mJ by interposing a half-wave plate between cross polarizers. The excitation beam and the probe beam generated by a pulsed xenon source were perpendicular to each other inside of the $1 \times 1 \text{ cm}$ cell. The analyzing beam was spectrally dispersed by a monochromator and converted to an electric signal by a Hamamatsu R 928 PM tube. The electric signal was recorded by a digital memory oscilloscope (Tektronix TDS 620 B) connected to a PC computer. The transient signals were analyzed by an in-house routine using Igor procedure. The reported decays and rate constants are the mean values of at least 10 different measurements.

3. Results and Discussion

Synthesis. Scheme 2 outlines the synthesis of the ligand **L1**. We based our strategy on the classical reaction between 1,2-bis(dichlorophosphano)ethane and the Grignard derivative of the commercially available 4-bromotrimethylsilylphenylacetylene, **2**. The oxidation step of phosphorus atoms was performed in the presence of H_2O_2 and was followed by the desilylation reaction. The phosphane oxide, **3**, was isolated in 26% yield over three steps. This intermediate key had already been prepared by our group and used for the preparation of other fluorophores.¹³ The Sonogashira²² cross-coupling between the phosphano product **3** and the iodide **4** (obtained easily by

SCHEME 2: Synthesis of Ligand L1^a



^a (a) Mg, THF, 50°C, 1.5 h then $\text{Cl}_2\text{PCH}_2\text{CH}_2\text{P}(\text{Cl})_2$, THF, RT, 20 h, 26%; (b) H_2O_2 , $\text{CH}_2\text{Cl}_2/\text{MeOH}$, RT, 100%; (c) K_2CO_3 , $\text{MeOH}/\text{CH}_2\text{Cl}_2$, RT, 4h, 80%; (d) 3 mol % $\text{Pd}(\text{PPh}_3)_4$, 6 mol % CuI, $1\text{-C}_6\text{H}_4\text{-O}(\text{CH}_2)\text{CO}_2\text{Et}$ **4**, Et_3N , toluene, 50°C, 56%.

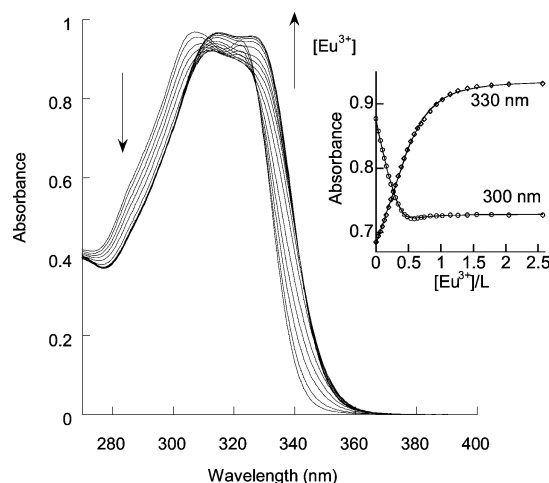
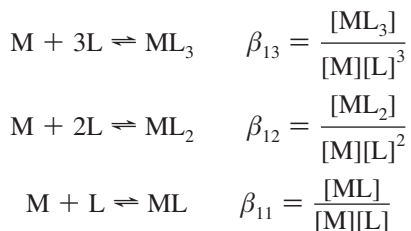


Figure 1. Absorption of ligand **L1** ($7.01 \times 10^{-6} \text{ M}$) in the presence of increasing concentration of Eu^{3+} in $\text{CH}_3\text{CN}/\text{CHCl}_3$ 8:2 v/v. Inset: Variation of the absorbance at 300 and 330 nm upon europium addition.

reacting iodophenol and bromoethylethanoate under basic conditions) was then performed in the presence of 3 mol % of Pd catalyst and 6 mol % of copper iodide. This reaction allowed the introduction of the desired aryl group, leading to the phosphane oxide ligand **L1** in 56% isolated yield. Having in hand such a bidentate derivative, we next studied complexation and photophysical properties of the europium complex.

Complexing Properties. The complexation studies of europium and terbium with **L** were performed in $\text{CH}_3\text{CN}/\text{CHCl}_3$ (8:2 v/v) in order to have a good dissociation of the rare earth salt and a good solubility of the complexes. The evolution of the absorption upon europium complexation is shown in Figure 1. Europium complexation induces a bathochromic shift of the absorption, which may be rationalized by an enhancement of the electron-withdrawing character of the phosphane oxide group due to the interaction of the oxygen atom with the cation. Careful analysis of the absorption spectra upon increasing europium addition by means of the SPECFIT program reveals that different complexes are formed with the following stoichiometry, ML , ML_2 , ML_3 . Analyses of the corresponding data gave the following values for the global association constants: $\log \beta_{13} = 20.80 \pm 0.2$; $\log \beta_{12} = 15.60 \pm 0.2$; and $\log \beta_{11} = 8.4 \pm 0.13$, which are defined by the following equations



We then turned our attention to the characterization of the photophysical properties of the europium complex. We have chosen the concentration conditions in which EuL_3 is the predominant species. As shown in Figure 2, under an excitation at 324 nm, the wavelength where Eu^{3+} is not absorbing, a strong quenching of the ligand emission was observed upon europium complexation together with the appearance of sharp peaks associated with ${}^5\text{D}_0 \rightarrow {}^7\text{F}_J$ and ${}^5\text{D}_1 \rightarrow {}^7\text{F}_J$ ($J = 0-4$) transitions characteristic of the europium luminescence.²³ The fluorescence quantum yield of the lanthanide ion was found to be 1%. The fluorescence of the ligand in the europium complex still remained, and the fluorescence quantum yield was found to be 2.5%. Such a value must be compared with the fluorescence quantum yield of the free ligand ($\Phi_{\text{F}} = 20\%$). We have also examined the complexation with the terbium ion. A quenching of the ligand fluorescence is observed, but no specific emission of the terbium is observed, which excludes the energy-transfer process from the ligand to the cation. Since electron transfer from the ligand to the terbium ion is thermodynamically forbidden, the observed quenching is due to the heavy atom effect, which enhances intersystem crossing. We have therefore used this complex TbL_3 as a reference compound to evaluate the heavy atom effect in the europium complex.

In order to further evaluate the photophysical properties of this new complex, time-resolved fluorescence measurements were performed by the single-photon counting method with picosecond laser excitation. The fluorescence decays of the ligand and its complex ML_3 with europium are shown in Figure 3. The decays are satisfactorily fitted by considering three decay times ($\tau_1 = 4.5$ ns, $\alpha_1 = 0.02$; $\tau_2 = 0.45$ ns, $\alpha_2 = 0.5$; and $\tau_3 = 0.01$ ns, $\alpha_3 = 0.48$) for **L1** ligand. As previously observed for the multichromophoric phosphane oxide ligand analogues,¹³ this effect can be explained by the presence of two different conformers; one may envisage the presence of an expanded structure leading to monomer emission ($\tau_2 = 0.45$ ns) and a near-sandwich geometry which allows the formation of an

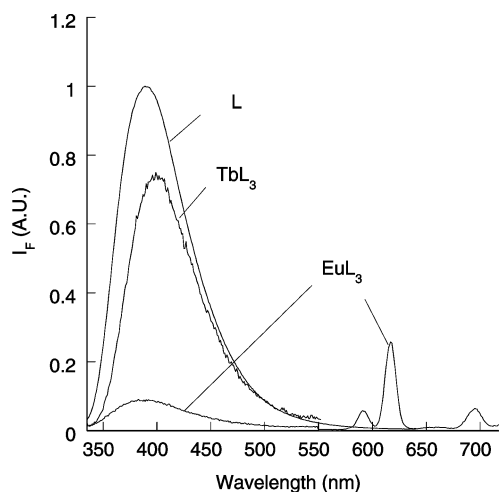


Figure 2. Corrected emission spectra of ligand **L1** (1.4×10^{-6} M) and its complexes EuL_3 and TbL_3 ; $\lambda_{\text{exc}} = 324$ nm.

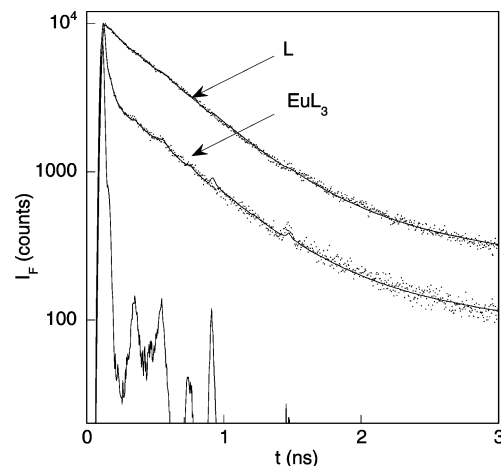


Figure 3. Fluorescence decays of **L1** (1.4×10^{-6} M) and its complex ML_3 with europium in $\text{CH}_3\text{CN}/\text{CHCl}_3$ 8:2 v/v. Channel width: 4.5 ps. Excitation wavelength: 323 nm. Emission wavelength: 400 nm.

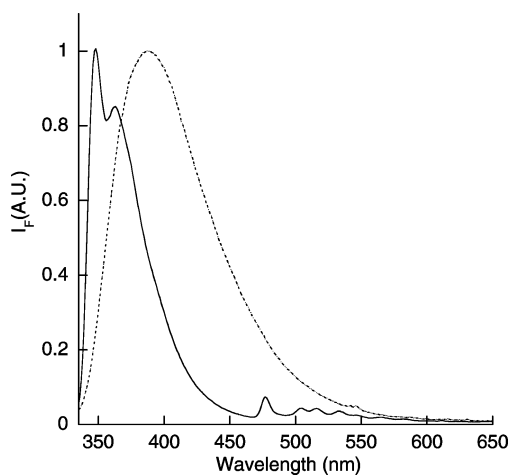


Figure 4. Luminescence of **L1** (1.4×10^{-6} M) in EtOH/MeOH 4/1 (v/v) at room temperature (dotted line) and at 77 K (solid line) ($\lambda_{\text{exc}} = 325$ nm).

excimer due to interactions between the chromophores in the excited state ($\tau_1 = 4.5$ ns, $\tau_3 = 0.01$ ns). By complexation with europium, a strong decrease of the fluorescence decay time at 430 nm was observed. For the ML_3 complex, satisfactory analysis of the fluorescence decay can be obtained by considering the following decay times ($\tau_1 = 0.02$ ns, $\alpha_1 = 0.84$; and $\tau_2 = 0.45$ ns, $\alpha_2 = 0.16$). The average decay time, which is defined as $\langle \tau \rangle = \sum_i \alpha_i \tau_i$, decreases from 0.31 to 0.088 ns upon complexation with Eu^{3+} . Such an effect is a consequence of either an energy transfer to the europium ion because of the spectral overlap between the absorption of the europium ion and the emission spectrum of the ligand or an electron transfer from the excited fluorophore to the Eu^{3+} . The electrochemical potential of the excited state of **L1** was determined ($E(\text{L}^+/\text{L}^*) = -2$ V/SCE) and clearly showed that the excited state of the ligand allows a reduction of the Eu^{3+} cation ($E = -0.35$ V/SCE). Such an electron transfer has already been reported for the interaction of Eu^{3+} with other fluorophores.²⁴

In order to evaluate the energy level of the triplet state of the ligand, we next examined its luminescence in a rigid matrix (EtOH/MeOH , 4:1 v/v) at 77 K. As observed in Figure 4, a structured and sharp band is observed with a maximum at 346 nm; this can be easily attributed to the ${}^1\text{LE}$ band instead of the CT band.²⁵ In addition, a weak structured band is observed between 460 and 650 nm, which can be attributed to the

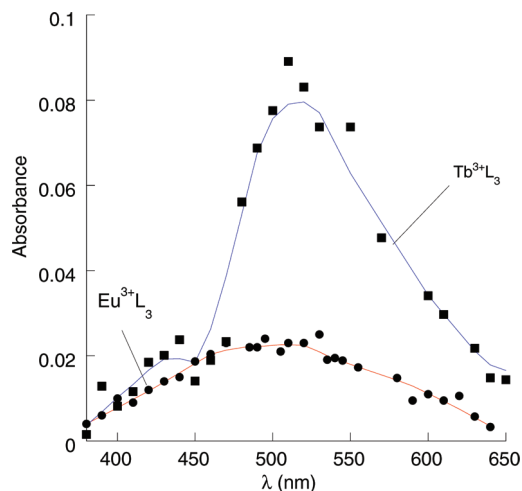


Figure 5. Normalized transient absorption spectra of the complexes of **L1** with Eu^{3+} and Tb^{3+} (Eu^{3+}L_3 and Tb^{3+}L_3 , respectively) in $\text{CH}_3\text{CN}/\text{CHCl}_3$ 8:2 v/v (nitrogen-saturated, obtained 10 ns after nanosecond laser excitation at 355 nm).

TABLE 1: Photophysical Data

compound	L1 ^a	EuL_3 ^a	TbL_3 ^a
Φ_{F} (%) ^b	20	2.5	15
$\langle\tau\rangle$ (ns) ^c	0.31	0.088	
Φ_{T} (%) ^b		7	
τ_{T} (μs)	4.5 ± 0.5	0.5 ± 0.1	1.7 ± 0.2

^a Measured in $\text{CHCl}_3/\text{CH}_3\text{CN}$ 20/80. ^b Errors: $\pm 10\%$.

^c Fluorescence average decay time of the ligand defined as $\langle\tau\rangle = \sum_i \alpha_i \tau_i$.

phosphorescence of the triplet state, and from the threshold of this band, the energy of this state has been estimated to be 21000 cm^{-1} . Thus, energy transfer is possible from the triplet state of the ligand to the ^5D states of the europium.

Further experiments have been made in order to characterize the energy transfer between the ligand and the europium. Transient absorption and emission experiments have been performed by using the third harmonic of a nanosecond Nd/YAG laser. The absorption spectrum of the triplet of ligand **L1** cannot be determined because of the low absorption of the fundamental at 355 nm. The triplet absorption spectra of the complex with Eu^{3+} and Tb^{3+} are displayed in Figure 5, and they exhibit a maximum at 505 and 540 nm, respectively. It should be noticed that the absorbance of the triplet of the ligand in the europium complex is significantly lower than that in the terbium complex. In fact, in both of these complexes, the intersystem conversion S_1-T_1 is accelerated due to a spin-orbit coupling enhancement produced by a heavy atom effect. The lower absorbance observed in the case of the europium complex is the consequence of an efficient quenching process from the excited singlet state by energy or electron transfer. The intersystem-crossing quantum yield Φ_{isc} was determined by studying the triplet energy transfer between the europium complex and benzophenone.²⁶ The Φ_{isc} for the ligand in the europium complex was found to be 0.07, which means that the most efficient nonradiative pathway from the singlet excited state occurs via electron or energy transfer to the europium.

The triplet lifetimes in a degassed and nitrogen-saturated solution have also been determined, and all of the photophysical data are gathered in Table 1. Upon complexation, a significant decrease of the triplet decay time of the ligand was observed for these two complexes, which may be rationalized again by an enhancement of the conversion T_1-S_0 by the spin-orbit

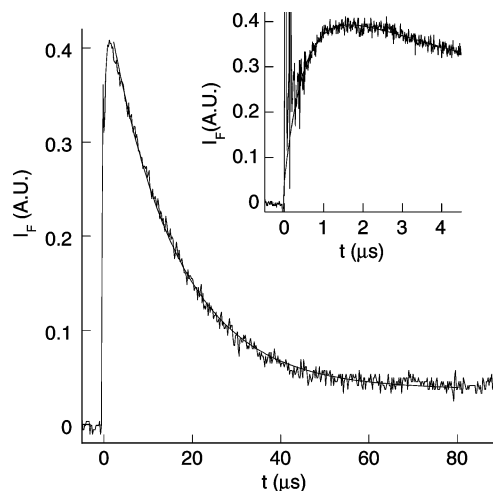


Figure 6. Time-resolved luminescence decays of the complex Eu^{3+}L_3 at $\lambda_{\text{em}} = 585 \text{ nm}$ ($\lambda_{\text{exc}} = 355 \text{ nm}$) in nitrogen-saturated $\text{CHCl}_3/\text{CH}_3\text{CN}$ 80/20 v:v.

coupling in the presence of a heavy atom. However, this decrease is more pronounced for europium complexation than for terbium complexation, which can be explained by an efficient energy transfer between the triplet state of the ligand and europium ion.

We then examined the kinetics of the europium luminescence in the complex by using a nanosecond laser and by excitation of the ML_3 complex at 355 nm. On the submillisecond time scale, by observing the $^5\text{D}_1$ emission at 585 nm, a decay time of $15 \pm 2 \mu\text{s}$ was observed (Figure 6). In order to improve the accuracy of the fast rise time, the fluorescence signal of the complex (EuL_3) was recorded on a shorter time scale (inset of Figure 6). A typical rise of the europium luminescence was observed, which was strongly disturbed by the ligand fluorescence. In the analysis, the longer decay time was fixed at $15 \mu\text{s}$, and a rise time of $0.5 \pm 0.1 \mu\text{s}$ has been found. This rise time corresponds exactly to the lifetime of the triplet state of the EuL_3 complex in a N_2 -saturated solution, which corroborates an efficient energy transfer between the triplet state of the ligand to the $^5\text{D}_1$ level of the lanthanide. It should be pointed out that, as the triplet quantum yield of **L** in the europium complex is low (7%), the proportion of excited states of europium populated by energy transfer from this triplet state is obviously small.

In order to obtain further information on this energy-transfer process, the resulting rise time in the temporal evolution of the europium luminescence was examined under different concentrations of oxygen (a solution saturated with nitrogen, a solution saturated with oxygen, and a solution under air atmosphere). The observed luminescence signals are displayed in Figure 7, and after fitting these signals with biexponentials, the corresponding rise times are equal to $0.096 \pm 0.005 \mu\text{s}$ for an O_2 -saturated solution, $0.28 \pm 0.03 \mu\text{s}$ for an aerated solution, and $0.5 \pm 0.1 \mu\text{s}$ for a N_2 -saturated solution. The rise time, which becomes shorter as the oxygen concentration increases, is evidence of the triplet energy-transfer process.

Furthermore, it should be noticed that the fits of the different luminescence signals start at the same point, which is different from zero. This can be rationalized by the fact that the energy transfer from the ligand to the europium may also occur via the singlet state of the ligand, which has been already described by Wang in the case of europium complexes.²⁷ The proportion of the different energy-transfer pathways can be determined from the interpolation of the luminescence curves when t is equal to 0 (I_0). In a first approximation, we can estimate that $\Phi_{\text{ET}}^{\text{S}}/\Phi_{\text{ET}}^{\text{T}}$

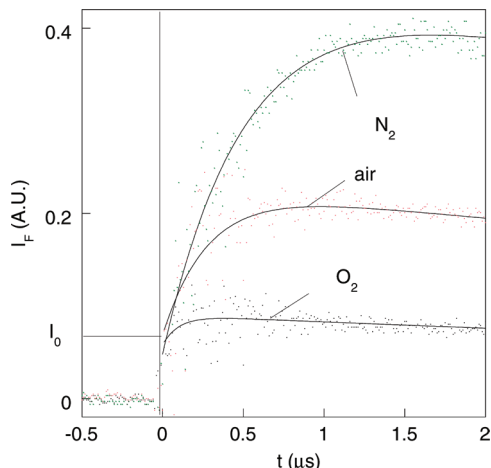


Figure 7. Time-resolved luminescence signals of the complex EuL_3 at $\lambda_{\text{em}} = 585 \text{ nm}$ ($\lambda_{\text{exc}} = 355 \text{ nm}$) in $\text{CHCl}_3/\text{CH}_3\text{CN}$ 80/20 v:v of a nitrogen-saturated solution, an oxygen-saturated solution, and an aerated solution.

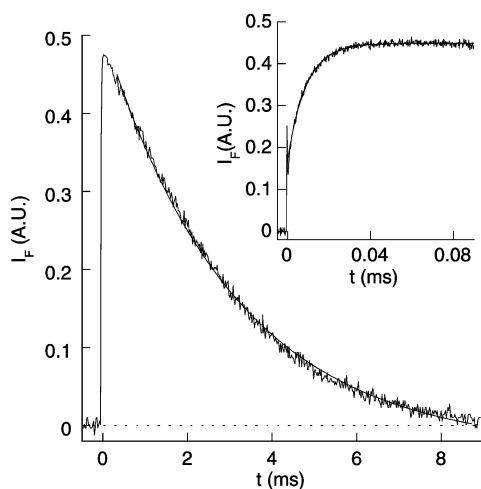


Figure 8. Time-resolved luminescence decays of the complex Eu^{3+}L_3 at $\lambda_{\text{em}} = 617 \text{ nm}$ ($\lambda_{\text{exc}} = 355 \text{ nm}$) in $\text{CHCl}_3/\text{CH}_3\text{CN}$ 80/20 v:v. Inset: time-resolved decay obtained with a smaller time scale.

$= 0.24$ (where $\Phi_{\text{ET}}^{\text{S}}$ and $\Phi_{\text{ET}}^{\text{T}}$ are the energy-transfer quantum yields from the first excited singlet and triplet states, respectively), which means that the energy transfer is four time more efficient from the triplet state than that from the singlet excited state. Going back to the different quenching processes of the first excited singlet state of the ligand, we may conclude that the energy-transfer process has a quantum yield which is lower than 2% (one-fourth of Φ_{ISC}), the electron-transfer process being therefore largely dominant.

We then focused on the study of the luminescence signals of the europium ion in the complex by exciting the complex at 355 nm. The populations of the $^5\text{D}_1$ and $^5\text{D}_0$ states were studied at around 600 nm (Figure 8). The obtained decay at 617 nm can be satisfactorily fitted by considering a decay time of $3.08 \pm 0.03 \text{ ms}$ and a rise time of $10 \pm 1 \mu\text{s}$, whereas the signal at 584 nm shows a decay time of $15 \pm 2 \mu\text{s}$ (inset of Figure 8). The rise time of the $^5\text{D}_0$ state is therefore in good agreement with the decay time of the $^5\text{D}_1$ state. Such an effect is completely consistent with a population of the $^5\text{D}_0$ state from the $^5\text{D}_1$ state as previously described by Van Veggel for other europium complexes.²⁸ From the luminescence decays obtained at different emission wavelengths, it has been possible to rebuild the luminescence spectrum of both states $^5\text{D}_1$ and $^5\text{D}_0$. The emission

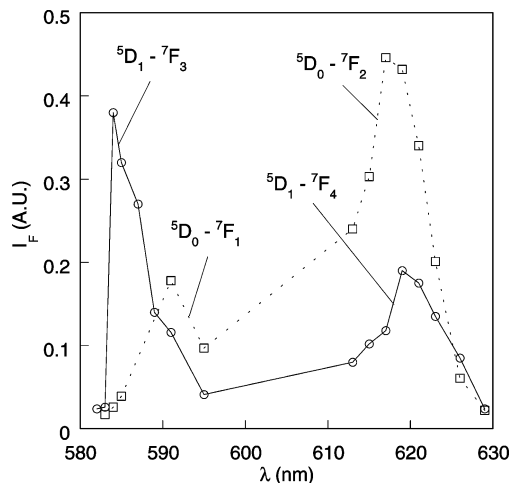
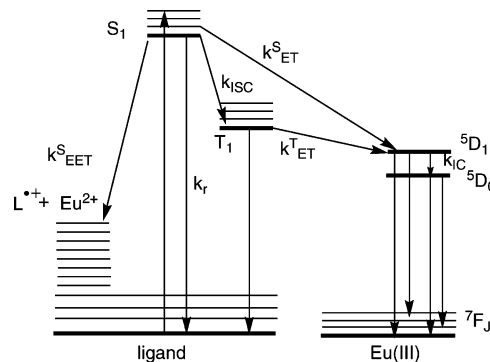


Figure 9. Emission spectra of $^5\text{D}_1$ and $^5\text{D}_0$ states of the Eu^{3+} complex; the solid line is associated with the $^5\text{D}_1$ curve (delay: $1 \mu\text{s}$), and the dashed line is associated with the $^5\text{D}_0$ emission (delay: $80 \mu\text{s}$) ($\lambda_{\text{exc}} = 355 \text{ nm}$). The involved transitions are indicated.

SCHEME 3: Schematic Diagram of the Photophysical Processes Leading to Sensitized Luminescence of the Ligand L



spectra of the $^5\text{D}_1$ and $^5\text{D}_0$ states are shown in Figure 9. The $^5\text{D}_1$ state has a maximum at 585 nm, whereas the $^5\text{D}_0$ state presents a maximum at 617 nm. The shapes of these emission spectra are in perfect agreement with those reported by Van Veggel for similar europium complexes.²⁸

4. Conclusion

In conclusion, we have synthesized a new phosphane oxide derivative able to efficiently sensitize the europium emission. It was shown that this ligand may interact with the trivalent europium ion, the stability constant of the resulting ML_3 complex being $\log \beta_{13} = 20.80 \pm 0.2$. Photophysical investigations of the complex were performed by stationary and time-resolved luminescence studies. The different pathways involved in the sensitization of the europium ion by the excited state of the ligand **L1** are shown in Scheme 3. The energy-transfer process occurs from both the singlet and the triplet states of the ligand **L1**. Additionally, the electron-transfer process leading to a charge separation ($\text{L}^{+\bullet} \text{Eu}^{2+}$) appears to be the most efficient deactivating pathway of the first excited singlet state of the ligand, which partially explains the relatively low luminescence quantum yield of the europium ion in the complex ($\Phi_{\text{F}} = 1\%$). The photophysical studies have shown that there is no direct energy transfer from the antenna to the $^5\text{D}_0$ state, but instead the $^5\text{D}_0$ state is populated via the $^5\text{D}_1$ state.

Acknowledgment. This work was supported by the Ministère de la Recherche program “ACI Jeunes Chercheurs 2004–2006”

and by the National Research Agency "CP2D program" 2008–2011. We are grateful to J.-P. Lefevre and J.-J. Vachon for their assistance in tuning the single-photon timing instruments. M.-H.H.-T. is grateful to the Ministère de la Recherche for a grant (2004–2007).

References and Notes

- (1) Bunzli, J. C. G.; Piguet, C. *Chem. Soc. Rev.* **2005**, *34*, 1048–1077.
- (2) Kido, J.; Okamoto, Y. *Chem. Rev.* **2002**, *102*, 2357–2368.
- (3) Sabbatini, N.; Guardigli, M.; Lehn, J. M. *Coord. Chem. Rev.* **1993**, *123*, 201–228.
- (4) (a) D'Aleo, A.; Pompidor, G.; Elena, B.; Vicat, J.; Baldeck, P. L.; Toupet, L.; Kahn, R.; Andraud, C.; Maury, O. *ChemPhysChem* **2007**, *8*, 2125–2132. (b) D'Aleo, A.; Picot, A.; Beeby, A.; Williams, J. A. G.; Le Guennic, B.; Andraud, C.; Maury, O. *Inorg. Chem.* **2008**, *47*, 10258–10268. (c) D'Aleo, A.; Picot, A.; Baldeck, P. L.; Andraud, C.; Maury, O. *Inorg. Chem.* **2008**, *47*, 10269–10267.
- (5) Coupez, B.; Boehme, C.; Wipff, G. *Phys. Chem. Chem. Phys.* **2002**, *4*, 5716–5729.
- (6) Charbonniere, L. J.; Ziessel, R.; Montalti, M.; Prodi, L.; Zaccheroni, N.; Boehme, C.; Wipff, G. *J. Am. Chem. Soc.* **2002**, *124*, 7779–7788.
- (7) Xu, H.; Yin, K.; Huang, W. *Chem.—Eur. J.* **2007**, *13*, 10281–10293.
- (8) Xu, H.; Yin, K.; Huang, W. *Chem. Phys. Chem.* **2008**, *9*, 1752.
- (9) Chauvin, A.-S.; Comby, S.; Baud, M.; De Piano, C.; Duhot, C.; Bunzli, J.-C. *Inorg. Chem.* **2009**, *48*, 10687–10696.
- (10) Xu, H.; Wang, L. H.; Zhu, X. H.; Yin, K.; Zhong, G. Y.; Hou, X. Y.; Huang, W. *J. Phys. Chem. B* **2006**, *110*, 3023–3029.
- (11) Ha-Thi, M. H.; Souchon, V.; Hamdi, A.; Metivier, R.; Alain, V.; Nakatani, K.; Lacroix, P. G.; Genet, J. P.; Michelet, V.; Leray, I. *Chem.—Eur. J.* **2006**, *12*, 9056–9065.
- (12) Metivier, R.; Amengual, R.; Leray, I.; Michelet, V.; Genet, J. P. *Org. Lett.* **2004**, *6*, 739–742.
- (13) Ha-Thi, M. H.; Penhoat, M.; Drouin, D.; Blanchard-Desce, M.; Michelet, V.; Leray, I. *Chem.—Eur. J.* **2008**, *14*, 5941–5950.
- (14) Ha-Thi, M. H.; Penhoat, M.; Michelet, V.; Leray, I. *Org. Lett.* **2007**, *9*, 1133–1136.
- (15) Ha-Thi, M. H.; Souchon, V.; Penhoat, M.; Miomandre, F.; Genet, J. P.; Leray, I.; Michelet, V. *Lett. Org. Chem.* **2007**, *4*, 185–188.
- (16) Ha-Thi, M. H.; Penhoat, M.; Michelet, V.; Leray, I. *Org. Biomol. Chem.* **2009**, *7*, 1665–1673.
- (17) D'Aleo, A.; Pompidor, G.; Elena, B.; Vicat, J.; Baldeck, P. L.; Toupet, L.; Kahn, R.; Andraud, C.; Maury, O. *ChemPhysChem* **2007**, *8*, 2125–2132.
- (18) Hasegawa, Y.; Yamamuro, M.; Wada, Y.; Kanehisa, N.; Kai, Y.; Yanagida, S. *J. Phys. Chem. A* **2003**, *107*, 1697–1702.
- (19) Demas, J. N.; Crosby, G. A. *J. Phys. Chem.* **1971**, *75*, 991–1024.
- (20) Boens, N.; Qin, W. W.; Basaric, N.; Hofkens, J.; Ameloot, M.; Pouget, J.; Lefevre, J. P.; Valeur, B.; Gratton, E.; Vandeven, M.; Silva, N. D.; Engelborghs, Y.; Willaert, K.; Sillen, A.; Rumbles, G.; Phillips, D.; Visser, A.; van Hoek, A.; Lakowicz, J. R.; Malak, H.; Gryczynski, I.; Szabo, A. G.; Krajcarski, D. T.; Tamai, N.; Miura, A. *Anal. Chem.* **2007**, *79*, 2137–2149.
- (21) Gampp, H.; Maeder, M.; Meyer, C. J.; Zuberbühler, A. D. *Talanta* **1985**, *32*, 95–101.
- (22) Chinchilla, R.; Najera, C. *Chem. Rev.* **2007**, *107*, 874–922.
- (23) Filipescu, N.; Sager, W. F.; Serafin, F. A. *J. Phys. Chem.* **1964**, *68*, 3324.
- (24) Inada, T.; Funasaka, Y.; Kikuchi, K.; Takahashi, Y.; Ikeda, H. *J. Phys. Chem. A* **2006**, *110*, 2595–2600.
- (25) Valeur, B. *Molecular Fluorescence. Principles and Applications*; Wiley-VCH: Weinheim, Germany, 2002.
- (26) *Flash Photolysis and Pulsed Radiolysis. Contributions to the Chemistry of Biology and Medicine*; Bensasson, R. V., Land, E. G., Truscott, T. G., Eds.; Pergamon Press: Paris, 1983.
- (27) Yang, C.; Fu, L.-M.; Wang, Y.; Zhang, J.-P.; Wong, W.-T.; Ai, X.-C.; Qiao, Y.-F.; Zou, B.-S.; Gui, L.-L. *Angew. Chem., Int. Ed.* **2004**, *43*, 5010–5013.
- (28) Klink, S. I.; Hebbink, G. A.; Grave, L.; Oude Alink, P. G. B.; van Veggel, F. C. J. M.; Werts, M. H. V. *J. Phys. Chem. A* **2002**, *106*, 3681–3689.

JP909402K